Welding in the World (2023) 67:89–97
https://doi.org/10.1007/s40194-022-01427-w

RESEARCH PAPER

Direction-independent laser-GMA hybrid welding with coaxial wire feed and annular beam

Michael Clemens[1] · **Lucas Warnecke**[1] · **Simon Olschok**[1] · **Uwe Reisgen**[1] · **Max Fabian Steiner**[2]

Received: 15 August 2022 / Accepted: 20 November 2022 / Published online: 3 December 2022

Abstract

Conventional laser gas metal arc hybrid welding (LB-GMA hybrid welding) is used as an efficient joining process in several high-tech steel processing production facilities. However, the use of the LB-GMA hybrid welding is often limited to the joining of linear weld seams as the welding process has a preferred welding direction due to lateral positioning of the laser beam and welding wire electrode. Reorienting the welding direction, therefore, often results in weld defects since changing the welding direction also requires a geometric manipulation of the GMA torch in relation to the laser beam optics. This means a considerable additional effort that is necessary if this efficient welding process is to be used for geometrically complex weld seam contours. Furthermore, the conventional LB-GMA hybrid welding process has a high adjustment complexity. Within this work, a direction-independent laser GMA hybrid welding head with an annular beam and coaxial wire feed is used. The annular laser beam with homogenous intensity profile is formed by a special processing head, split and reassembled around the coaxial wire. Due to the coaxial arrangement of the wire electrode to the annular beam, the hybrid process is in theory direction independent. As a result, there should not be any irregularities in the weld seam, when the welding direction is changed. The annular beam considerably reduces the complexity of adjustment and improves reproducibility. The focus of this work is to qualify the process for joining geometrically complex weld contours and to investigate possible advantages of the directional independence of the coaxial LB-GMA hybrid welding process. For this purpose, fillet welds in lap joint configuration with a sheet thickness of 2 mm each at different weld contours (different direction changes, corners, radii) are discussed. By performing a DoE-based sensitivity analysis, influencing factors on the quality of the generated weld are analysed.

Keywords Laser beam welding · Gas metal arc welding · Hybrid welding · Direction-independent laser-GMA hybrid welding · Coaxial laser-GMA hybrid welding · Annular laser beam · Coaxial wire feed

1 Introduction/motivation

Hybrid processes of laser beam and arc welding have been known for more than 40 years [1, 2]. A characteristic feature of these processes is the joint action of laser beam and arc in a common process zone. Combinations of two or more energy sources are described as hybrid processes. The combined processes can be distinguished in serial or hybrid processes. In hybrid processes, the coupling of two individual processes leads to synergy effects. In this context, synergy effects are defined as an increased penetration depth or an increased welding speed, as the results of various research projects have shown [3]–[6].

Conventional laser-gas metal arc hybrid welding (LB-GMA hybrid welding) is used as an efficient joining process in some high-tech steel processing production facilities [7]–[9]. Due to the high degree of automation as well as the high achievable welding speed, considerable economic advantages can be generated compared to conventional arc welding processes [10].

However, the conventional LB-GMA hybrid welding process is often limited to joining linear weld seams since

Recommended for publication by Commission IV - Power Beam Processes

✉ Michael Clemens
michael.clemens@isf.rwth-aachen.de

[1] Welding and Joining Institute, RWTH Aachen University, Pontstraße 49, 52062 Aachen, Germany

[2] Fraunhofer Institute for Laser Technology ILT, Steinbachstraße 15, 52074 Aachen, Germany

the hybrid process is direction dependant due to the lateral positioning of the laser beam and welding wire electrode. Reorientation of the welding direction (especially for small radii) without resetting the working point of the GMA torch relative to the laser beam working point (considerable effort) leads to significant weld irregularities [11]. Furthermore, the conventional LB-GMA hybrid welding process has a high adjustment complexity due to the lateral positioning of the laser beam relative to the GMA torch. In addition to various arc- and laser beam–specific adjustment parameters, the hybrid coupling of the two individual processes results in further geometric adjustment parameters (leading/trailing laser beam, process distance, angle of attack of laser beam, and GMA torch, for example). Even small deviations in the mentioned geometric adjustments lead to significant changes in the resulting weld quality [11].

To extend the application of the LB-GMA hybrid welding process for joining complex weld seam geometries and to simultaneously reduce the geometric adjustment complexity of the hybrid process, a processing head for coaxial laser arc (COLLAR) hybrid welding and additive manufacturing with wire was developed at the Fraunhofer Institute for Laser Technology (ILT) [12].

In unpublished preliminary tests, the novel COLLAR hybrid welding process was adjusted for blind welds on 10-mm sheet mild steel. In Fig. 1, an example of arc only and the COLLAR hybrid welding process is depicted.

The characteristic features of the hybrid weld, resulting from the synergy effects due to coupling of the two individual processes—wider and deeper penetration geometry compared to the arc weld—could be demonstrated with the newly developed COLLAR hybrid welding head. In addition to these initial, fundamental investigations, videographic images were taken with a high-speed camera to expand the understanding of the process.

2 Welding setup

In the newly developed COLLAR hybrid welding head, the laser beam welding process and the GMA welding process are coaxially aligned and combined in a common working point. The wire electrode is positioned concentric to the annular laser beam. Consequently, only the focussing length of the annular laser beam, the concentricity between the annular beam and the GMA wire electrode, and the stickout of the GMA burner remain as geometrically adjustable process parameters. Figure 2a depicts the sketch of the hybrid process. In addition, Fig. 2b shows the optical components of the COLLAR hybrid welding head and the associated beam shaping principle, which forms an annular beam from a single collimated laser beam. Figure 2c depicts the experimental setup with the mounted COLLAR hybrid welding head at the Welding and Joining Institute at RWTH Aachen University (ISF).

Figure 3a defines the laser level E_L. The laser level E_L describes the perpendicular distance of the reference point inscribed on the COLLAR hybrid head to the workpiece and is abbreviated with unitless digits. Laser level $E_L = 32$, for example, represents the near-focus area; larger laser levels display defocussed welding. The larger the selected laser level, the more defocussed the laser beam and thus the geometrically larger the laser beam ring imaged on the workpiece. Figure 3b illustrates the beam caustic with two different laser levels drawn in. Laser level $E_L = 40$ thus means a laser ring with an inner diameter of approx. 2.5 mm imaged on the workpiece. By focusing (and thus increasing the distance between the reference point on the COLLAR hybrid head and the workpiece by 5 mm), the laser level $E_L = 30$(inner diameter of the laser ring of approx. 0.3 mm) is imaged on the workpiece. The irradiated area (red area) and the resulting dimensions and

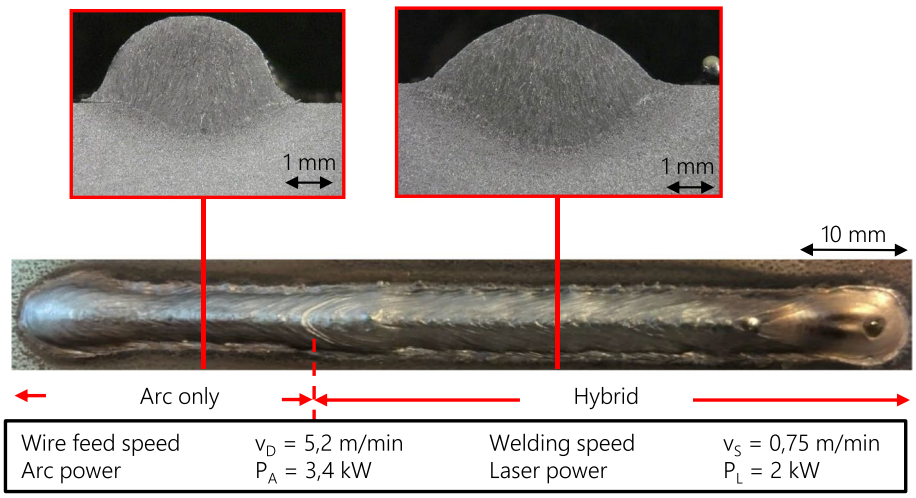

Fig. 1 Comparison of arc only (left side) and hybrid welding (right side)

geometries of the laser beam rings are shown schematically in Fig. 3c.

A Qineo Next 452 Premium from Cloos is used as the GMA power source. When varying the wire feed in the range of 5–6 m/min, a constant voltage short arc is established. The stickout was constant at 12 mm throughout all welding trials. The minidrive system developed at ISF operates as an external wire feed system to be able to manipulate the wire feed independently of the current set on the power source.

A disk laser with a maximum output power of 16 kW is used as the laser beam source (TruDisk 16,002; Trumpf; beam quality: 8 mm*mrad). The optical setup of the hybrid welding head has a focussing focal length of $f_f = 120$ mm and a collimation focal length of $f_c = 100$ mm. An optical fibre with a fibre diameter of 200 µm is used.

In the welding tests, a mild steel of grade S355JR (EN10025-2 [13]) with a sheet thickness of 2 mm is employed as base material. The wire electrode is a copper-plated G3Si1 (G42 4 M21 3Si1 [14]) with a diameter of 1.2 mm. The chemical compositions of the base material and wire electrode are listed in Table 1.

The used shielding gas is a mixed gas of 82% argon and 18% carbon dioxide. The joining partners are arranged in lap joint configuration with a sheet thickness of 2 mm in each case and executed as a fillet weld.

After the welding tests have been carried out, the weld specimens are measured three dimensionally with the aid of a confocal microscope, and a topography measurement record of the generated weld is created. This allows for the height measurement values to be analysed before, in, and after the direction change.

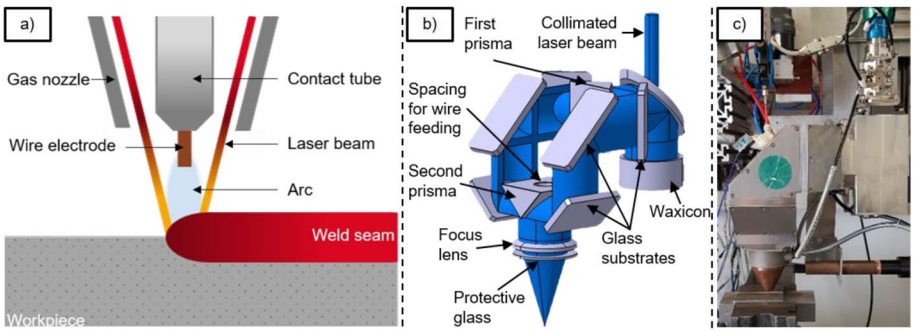

Fig. 2 Process zone, schematic (**a**); Beam shaping principle of the COLLAR hybrid welding head [12] (**b**); Experimental setup with the COLLAR hybrid welding head (**c**)

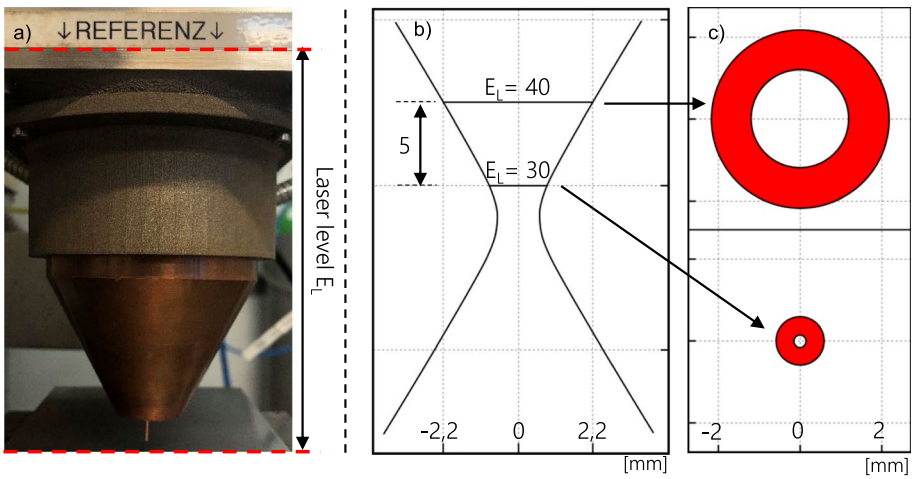

Fig. 3 Definition laser level E_L (**a**); The beam caustic COLLAR hybrid welding head with depicted laser levels (**b**); Dimensions and geometry of different laser rings, schematically (**c**)

Table 1 Chemical composition base material and wire electrode (mass %), measured by OES[1] analysis

	Designation	C [%]	Si [%]	Mn [%]	P [%]	S [%]	Ni [%]	Cu [%]
Basic material	S355JR	0.064	0.023	1.33	0.01	0.001	0.013	0.017
Wire electrode	G3Si1	0.06–0.14	0.7–1.0	1.3–1.6	0.025	0.025	0.15	0.35

[1] *OES*, optical emission spectroscopy

3 Results/discussion

Based on the previous fundamental process understanding that could be generated in the joining of blind welds, a design of experiments (DoE) is carried out to qualify the COLLAR hybrid welding head for the joining of fillet welding in lap joint configuration in the thin sheet area. The results of these first tests serve as the basis for the second test step, in which basic directional changes such as angles and radii are investigated. In the following third step, these basic directional changes are extended to more complex weld seam geometries. In the last step of the test series, the increase of the welding speed from 2 to 3 m/min is investigated. Subsequently, the weld seams produced are analysed with regard to their external and internal weld seam quality using a confocal microscope and macroscopic cross sections.

3.1 Transfer of the process understanding to fillet weld in lap joint configuration

To transfer the process understanding gained for blind welds to the joining of fillet weld in lap joint configuration, a design of experiments (DoE) is carried out in the first step. With this method, the interdependencies between the welding parameters (designated as factors in the following) and the qualitative and quantitative characteristics of the weld seam (designated as quality characteristics in the following) can be investigated and analysed in a resource-saving manner. The experimental plan in the face-centred central composite design was designed and evaluated with Minitab® [15]. In one base block, it comprises 16 cube points, ten axial points, and one centre point.

Commercially available power sources with integrated wire feed devices (such as the Qineo Next 452 Premium used) for GMA welding have internal characteristic curves that calculate suitable welding voltage and current values for the set wire feed so that a stable welding process is made possible. For the LB-GMA hybrid test setup used, an external wire feed device is applied, whose parameter wire feed speed minidrive v_{DM} is defined relative to wire feed speed power source v_D. The parameter v_D thus defines the current and voltage values of the arc via the internal characteristic curve of the power source, while the wire feed is determined and set independently by v_{DM}.

The factors of the DoE and their value ranges are listed in Table 2. Included are the welding speed v_S as the basic process parameter, as well as the wire feed speed power source v_D and the laser power P_L, which define the amount of energy introduced by the two individual processes. In addition, the laser level E_L, which was explained in the previous chapter, is examined within the DoE. The wire feed speed minidrive v_{DM} of the minidrive wire feed system is varied and is set relative to the wire feed speed power source v_D.

Table 2 Factors and value ranges of the DoE

Factor	Symbol	Minimum	Maximum
Welding speed	v_S	2 m/min	3 m/min
Wire feed speed power source	v_D	5.2 m/min	7.6 m/min
Laser power	P_L	2 kW	3 kW
Laser level	E_L	32	37
Wire feed speed minidrive	v_{DM}	100%	115%

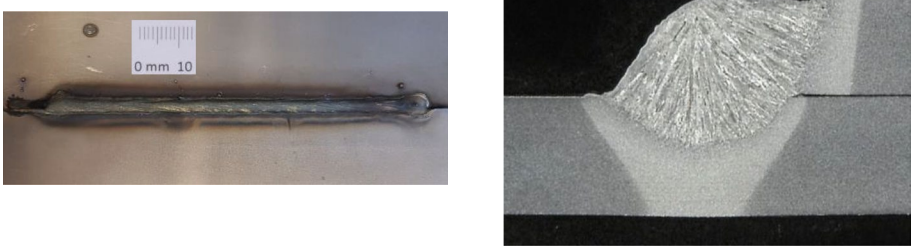

a) Photographic image, linear seam, 2 m/min

b) Macroscopic image, linear seam, 2 m/min

Fig. 4 Photographic image of the seam (**a**); Macroscopic cross section image of the weld seam (**b**)

Table 3 Measured quality characteristic of the DoE

Quality characteristics	Number	Unit
Welding current	1	A
Welding voltage	2	V
Arc power	3	W
Depth burn-in notch	4	mm
Width burn-in notch	5	mm
Penetration depth lower sheet	6	mm
Welding width lower sheet	7	mm
Symmetry auxiliary dimension	8	–

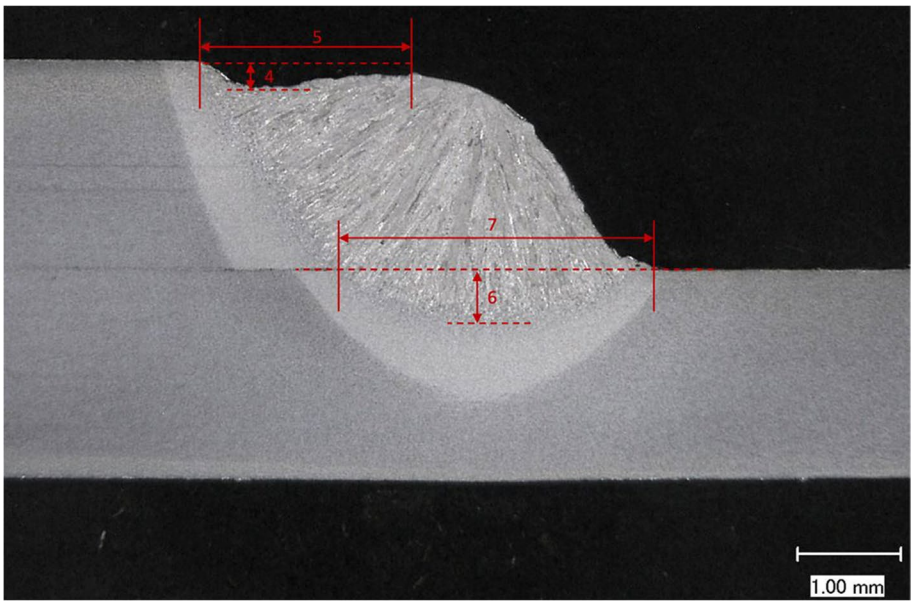

Fig. 5 Overview of quality characteristics in macroscopic cross section

The welding tests are evaluated regarding various quality characteristics. The selection of quality characteristics is based on the valid standards (DIN EN ISO 6520 [16], DIN EN ISO 12932 [17]) for irregularities in fusion-welded joints. Furthermore, process-specific quality characteristics as the measured arc power are also evaluated.

The quality characteristics welding current and welding voltage as well as the resulting arc power are mainly used to verify the evaluation. All expected significant effects of the wire feed speed power source v_D could be demonstrated (such as the positive effect of the wire feed speed power source v_D on arc power).

The continuous burn-in notch (clearly visible in Fig. 4b) (order no. 5011 according to DIN EN ISO 6520), which was always formed in the weld seams, is only permissible up to a depth of $k \leq 0.05\ t$ ($t \triangleq$ sheet thickness) according to evaluation group B of DIN EN ISO 12932. Evaluation group C allows a depth of the burn-in notch of $k \leq 0.1\ t$, but a maximum of 0.5 mm, whereas evaluation group D even allows a depth of $k \leq 0.2\ t$, but a maximum of 1 mm. Applied to the used sheet thickness of 2 mm, this results in a maximum penetration depth of 0.1 mm for evaluation group A, 0.2 mm for evaluation group B, and 0.4 mm for evaluation group C. Only three of the 27 samples fall below the required 0.4 mm for evaluation group D. The depth and the width of the burn-in notch were, therefore, included in the DoE as a quality characteristic.

The further quality characteristics describe the bonding and the symmetry of the weld seam. In addition to the weld penetration depth and the weld width in the lower sheet, this also

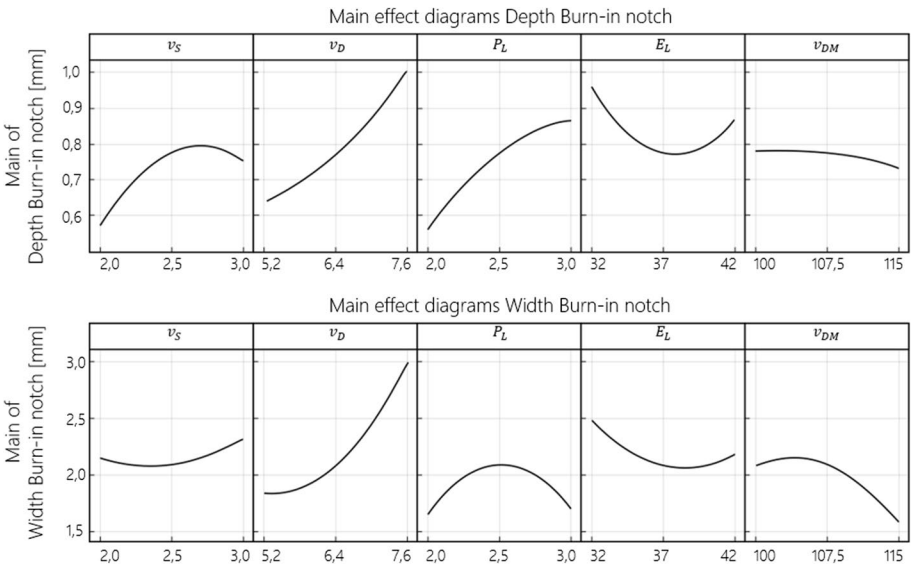

Fig. 6 Main effect diagrams depth burn-in notch (**a**); Main effect diagrams width burn-in notch (**b**)

Table 4 Parameters for the test series to validate the directional independence

Factor	Value
Welding speed v_S	2 m/min
Wire feed speed power source v_D	5.2 m/min
Laser power P_L	2 kW
Laser level E_L	32
Wire feed speed minidrive v_{DM}	115%

includes the auxiliary symmetry dimension (defined in DIN EN ISO 12932), which quantifies the symmetry of the weld seam.

The quality characteristics are listed in Table 3, including their corresponding numbers and units.

Figure 5 shows the quality characteristics numbers 4 to 7 in the macroscopic cross section of the weld.

For the evaluation of the DoE, the significance level α is set to the value of 0.05 established in engineering sciences. This means that the risk of falsely recognising an effect is 5%. An effect is, therefore, significant if its significance value is below the significance level. [18] Of particular interest are the main effects, as the factors can be directly parameterised.

The complete evaluation of the DoE cannot be reproduced within the limited scope of this paper. The abbreviated evaluation, therefore, concentrates on the quality features that characterise the burn-in notch, as this is not standard compliant and acts as a notch in which stress peaks can occur under load.

For the quality characteristic depth burn-in notch, the three factors welding speed v_S, wire feed speed power source v_D, and laser power P_L are significant. The corresponding main effect diagrams can be seen in.

Fig. 6a. For the quality characteristic width burn-in notch, v_D is the only significant main effect, displayed in Fig. 6b. In addition, the interaction effect $v_S * v_D$ is significant.

The welding result presented here with the associated significant factors of the DoE serves as a basis for the selection of a suitable welding parameter set and for the subsequent investigations of the directional independence of the COLLAR hybrid welding head in the following chapter.

3.2 Welding of direction changes

Due to the special beam shaping concept and the coaxial arrangement, the GMA wire electrode is enclosed by the annular beam of the COLLAR hybrid welding head. In theory, this should result in a direction-independent welding process. Basic directional changes such as angles and radii

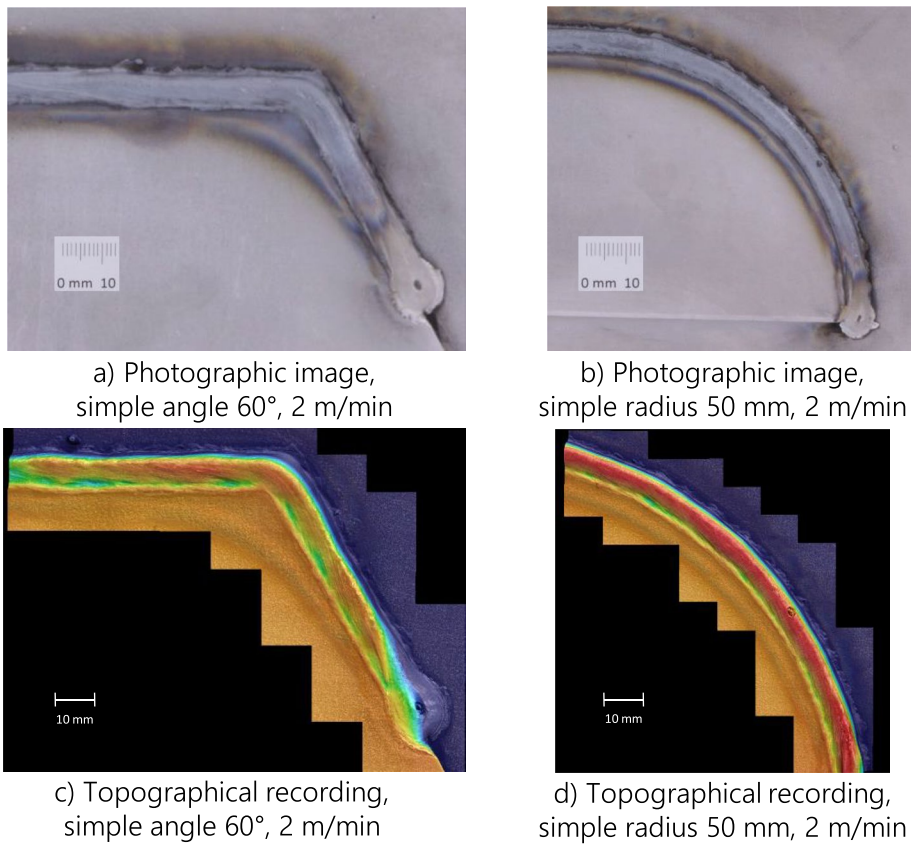

Fig. 7 Basic direction changes

a) Photographic image, simple angle 60°, 2 m/min

b) Photographic image, simple radius 50 mm, 2 m/min

c) Topographical recording, simple angle 60°, 2 m/min

d) Topographical recording, simple radius 50 mm, 2 m/min

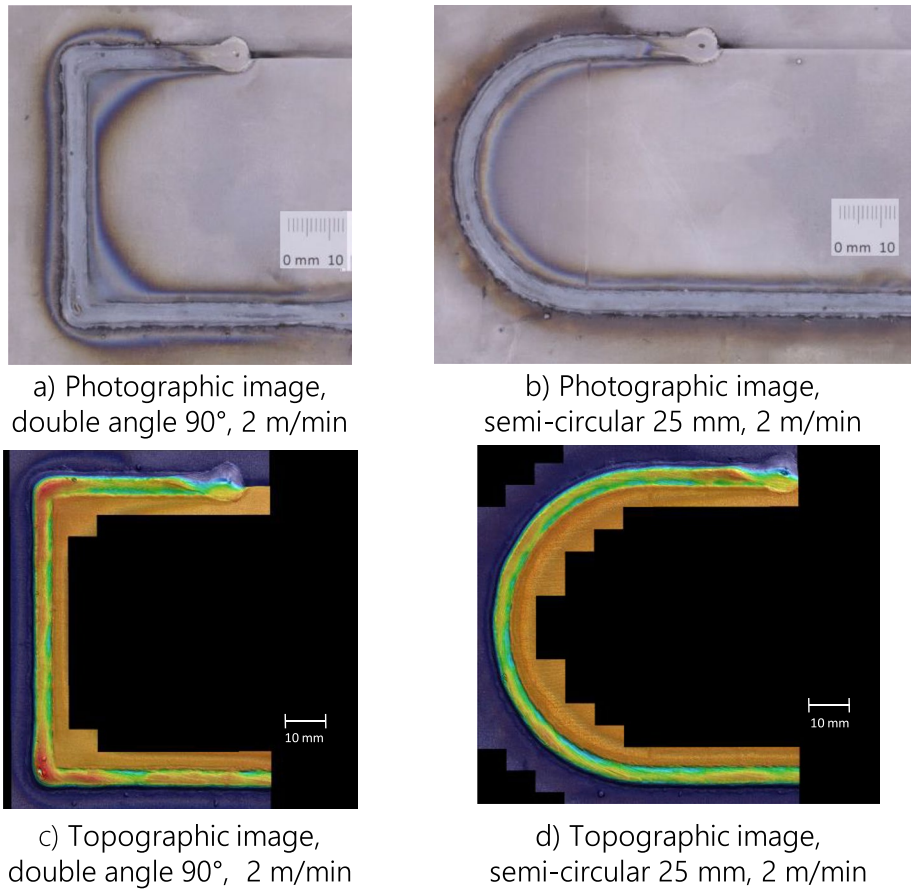

a) Photographic image, double angle 90°, 2 m/min

b) Photographic image, semi-circular 25 mm, 2 m/min

c) Topographic image, double angle 90°, 2 m/min

d) Topographic image, semi-circular 25 mm, 2 m/min

Fig. 8 Complex direction changes

can be considered as basic elements of any complex weld seam geometry. The parameters of the DoE obtained in the first step are now used in the second step of this series of experiments to investigate differently parameterised, basic directional changes.

Table 4 shows the standard welding parameters that were selected based on the preliminary tests from Sect. 3.1. The welds generated with the parameters are characterised by a high reproducibility with regard to the generated weld quality.

The basic directional changes investigated include angles from 15 to 120° in 15° increments and basic radii of 25-, 50-, and 75-mm radii. Figure 7 shows an angle with 60° as well as a radial direction change with a 50-mm radius.

With the basic direction changes, there are no irregularities in the geometrical shape of the weld top bead up to

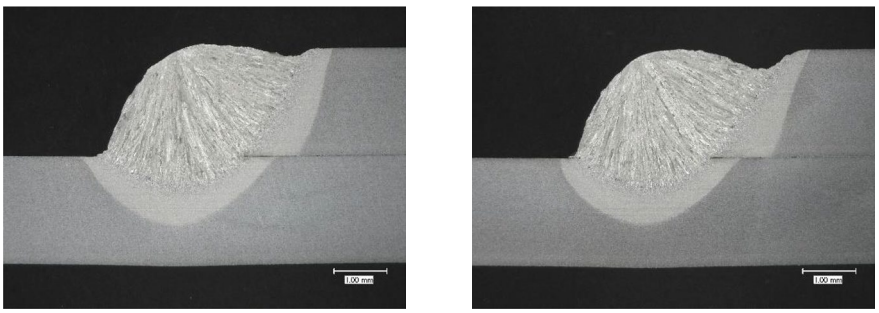

a) Macroscopic image before the change of direction, simple angle 15°, 2 m/min

b) Macroscopic image after the change of direction, simple angle 15°, 2 m/min

Fig. 9 Macroscopic images before and after the direction change

Table 5 Parameters for increasing the welding speed to 3 m/min

Factor	Value
Welding speed v_S	3 m/min
Wire feed speed power source v_D	5.2 m/min
Laser power P_L	3.5 kW
Laser level E_L	37
Wire feed speed minidrive v_{DM}	132%

an angle of 60°. From an angle of 75°, an increase of the weld reinforcement can be observed at the angular point of the direction change, which increases steadily up to the largest welded angle of 120°. It is assumed that this can be explained by the lack of power adjustment or speed variations at the angular point. The process continues at full power and full wire feed speed at the angle point, while the reorientation results in increasing reversal times and, thus, slower speeds at the angle point. With radial direction changes, the effect of weld super-elevation is not observed. It is suspected that this is because the absolute welding speed is constant during the continuous direction change.

The basic directional changes investigated in the second step can be combined in the third step to form more complex weld seam geometries. These include the combination of two angles of 90° each and the combination of two radii of 25 mm to a semi-circular weld seam, shown in Fig. 8.

The results obtained when welding complex direction changes match the results of the basic direction changes. In the case of the double angles, an increase of the weld reinforcement in the angular points of the direction changes can be observed. An increase in the weld reinforcement is not observed in the experiments with the semicircular seams.

The directional independence of the COLLAR hybrid welding head can also be verified with macroscopic cross sections in addition to the topographic representation of the welds.

Figure 9 shows macroscopic cross sections before (Fig. 9a) and after (Fig. 9b) the direction change. The only measurable difference is the deepened burn-in notch in the upper sheet in Fig. 9b.

In further welding tests, an increase of the welding speed from 2 m/min to 3 m/min could be achieved by adjusting the welding parameters. The adjusted welding parameters are depicted in Table 5.

As determined in the previous tests, geometrically uniformly shaped welds are produced over the entire complex weld contour, even after the welding speed is increased. In Fig. 10, photographic images of the two complex weld geometries are depicted.

Compared to the welding test depicted in Fig. 8a with a welding speed of 2 m/min, the photographic image in Fig. 10a clearly shows a reduced heat-affected zone around the two 90° direction changes. In the radial direction changes depicted in Fig. 10b, as already depicted in Fig. 8b, no geometrical irregularities in the weld contour are measured. A reason for this may again be the continuous direction change.

4 Conclusions

In this work, the directional independence of the COLLAR hybrid welding head has been demonstrated.

In the first step, the previous process understanding generated by simple blind welds was transferred to the fillet welding in lap joint configuration with a sheet thickness of 2 mm each. With the aid of a DoE-based sensitivity analysis, it was possible to identify interdependencies between the relevant welding parameters. Thereby, parameter sets for the quality-compliant and reproducible joining of the above-mentioned joining task could be set up.

In the second step, elementary directional changes such as angles and radii were successfully welded. Based on this, it was also possible to weld more complex weld seam geometries resulting from the composition of several basic directional changes in the third step.

The stability and the robustness of the COLLAR hybrid welding process before, in, and after direction changes

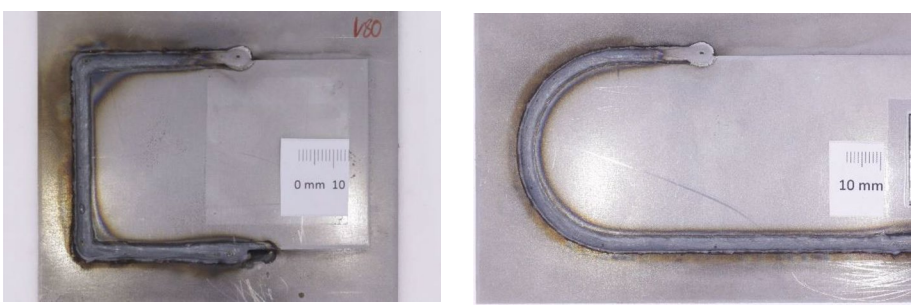

Fig. 10 Complex weld seam geometries with v_S= 3 m/min

a) Photographic image, double angle 90°, 3 m/min

b) Photographic image, semi-circular 25 mm, 3 m/min

could be demonstrated and measured by means of macroscopic cross sections and topographic images.

In the final step, the welding speed of the COLLAR hybrid welding process could be increased from 2 to 3 m/min by adjusting the welding parameters. No defects in the welded seams were observed or measured. Therefore, the new parameters are deemed suitable for welding and further use.

In future experiments, the welding speed must be further increased to achieve a highly efficient coaxial hybrid welding process. Furthermore, a qualification of the COLLAR hybrid welding process for thick sheet joining should be performed to open new use cases and to ensure the applicability of the COLLAR hybrid welding process across all sheet thickness areas.

Acknowledgements A further acknowledgement addresses to the DVS-IIW Young Professionals funding initiative for the financial and organisational support to attend the 75th IIW Annual Assembly and International Conference 2022 in Tokyo, Japan.

Funding Open Access funding enabled and organized by Projekt DEAL. The IGF project "RichtungsunabhängigesLaser-MSG-HybridschweißenmitRingfokus und koaxialerDrahtzuführungfür das Verbindungsschweißen und die additive Fertigung" IGF project no. 21.071 N of the Research Association on Welding and Allied Processes of the DVS, AachenerStraße 172, 40223 Düsseldorf, was funded by the AiF within the framework of the programme for the promotion of industrial joint research (IGF) of the Federal Ministry of Economics and Climate Protection on the basis of a decree of the German Bundestag.

Declarations

Conflict of interest The authors declare that they have no conflict of interest.

References

1. Eboo M, Steen M, Clarke J, Eds., (1978) "Arc-augmented laser welding". Met Constr 11:332–335
2. Matsuda J, Utsumi A, Katsumura M, Hamasaki M, Nagata S (1988) TIG or MIG arc-augmented laser welding of thick mild steel plate. Join Mater 1:31–34
3. Fuhrmann C, Petring D, Poprawe R (2005) Recent results on high power CO2- and Nd: YAG-laser-arc hybrid welding of thick steel plates. Lasers in manufacturing , LIM 2005, Munich, Germany, June 13th - 16th. Beyer E (ed) for the German Scientific Society (WLT) 185–192. https://www.llt.rwth-aachen.de/cms/LLT/Forschung/~dokg/Publikationen/?search=Recent+results+on+high+power+CO2-+and+Nd%3AYAG-laserarc+hybrid+welding+of+thick+steel+plates&page=
4. Thomy C et al (2003) "CO2-Laser-MSG-Hybridschweißen in der Rohrfertigung", DVS-Berichte 225. Schweißen Schneiden 2003:167–174
5. Mazar Atabaki M, Ma J, Yang G, Kovacevic R (2014) Hybrid laser/arc welding of advanced high strength steel in different butt joint configurations. Materials & Design 64:573–587. https://www.sciencedirect.com/science/article/abs/pii/S0261306914006244?via%3Dihub
6. Mahrle A et al (2011) Process charcacteristics of fibre-laser-assisted plasma arc welding. J Phys D Appl Phys 44(34):345502
7. Reutzel EW, Sullivan MJ, Mikesic DA (2006) Joining pipe with the hybrid laser-GMAW process: weld test results and cost analysis. Weld J 85(6):66–71
8. Olschok S, Reisgen U, Dilthey U (2007) "Robot application for laser-GMA hybrid welding in shipbuilding", in Proc. Of the Laser Materials Processing Conference ICALEO, pp. 308–315, Orlando
9. Walz C, Springer IS, El Rayes M, Seefeld T, Sepold G (2001) "Hybrid welding of steel for offshore applications", in Proc. Of the 11th International Offshore and Polar Engeneering Conference
10. Acherjee B (2018) Hybrid laser arc welding: state-of-the-art review. Opt Laser Technol 99:60–71
11. Kah P (2013) Overview of the exploration status of laser-arc hybrid welding processes. Rev Adv Mater Sci 2013(30):112–132
12. Steiner MF, Kelbassa J (2022) "Coaxial laser arc hybrid additive manufacturing with wire", AKL – International Laser Technology Congress. https://publica.fraunhofer.de/handle/publica/418449
13. DIN EN 10025–2:2019–10, Warmgewalzte Erzeugnisse aus Baustählen - Teil 2: Technische Lieferbedingungen für unlegierte Baustähle; Deutsche Fassung (EN 10025–2:2019)
14. DIN EN ISO 14341:2020–12, Schweißzusätze - Drahtelektroden und Schweißgut zum Metall-Schutzgasschweißen von unlegierten Stählen und Feinkornstählen - Einteilung (ISO 14341:2020)
15. Minitab LLC (2021) Minitab. Version 20.3. Retrieved from https://www.minitab.com/en-us/legal/author-permissions-guidelines/
16. DIN EN ISO 6520–1:2007–11. Schweißen und verwandte Prozesse - Einteilung von geometrischen Unregelmäßigkeiten an metallischen Werkstoffen - Teil 1: Schmelzschweißen (ISO 6520–1:2007); Dreisprachige Fassung EN ISO 6520–1:2007
17. DIN EN ISO 12932:2013–10. Schweißen - Laserstrahl-Lichtbogen-Hybridschweißen von Stählen, Nickel und Nickellegierungen - Bewertungsgruppen für Unregelmäßigkeiten (ISO 12932:2013); Deutsche Fassung EN ISO 12932:2013.
18. Siebertz K, van Bebber D, und Hochkirchen T (2017) Statistische Versuchsplanung. Berlin, Heidelberg: Springer Berlin Heidelberg